

*Full Length Research Paper*

# A combined high and low cycle fatigue model to estimate life of steel bridges

Kamal Karunananda<sup>1\*</sup>, Mitao Ohga<sup>1</sup>, Ranjith Dissanayake<sup>2</sup> and Sudath Siriwardane<sup>1</sup>

<sup>1</sup>Department of Civil and Environmental Engineering, Ehime University, Bunkyo-cho 3, Matsuyama 790-8577, Japan.

<sup>2</sup>Department of Civil Engineering, University of Peradeniya, Peradeniya 20400, Sri Lanka.

Accepted 26 July, 2010

**This paper proposes a new model to estimate life of structures for combined damage of high and low cycle fatigue. The model mainly consists of a new damage indicator and strain-life fatigue curve. The model predictions are verified by comparing with fatigue test results of some materials. The proposed model is applied to estimate the fatigue life of a bridge member for combined damage of high cycle and low cycle fatigue caused by usual traffic and earthquake loadings. Finally, the importance and applicability of the proposed model is confirmed.**

**Key words:** High cycle fatigue, low cycle fatigue, combined damage, railway, bridge.

## INTRODUCTION

Bridges are generally subjected to high cycle fatigue (HCF) caused by usual traffic loading (Chen, 1987). Recently, many fatigue failures of bridges have been reported in different parts of the world or to give similar idea. Some of these failures cannot be explained by HCF phenomenon alone. Studies of these failures reveal that overloading caused by earthquakes is one of the reasons for these incidents. When a bridge is subjected to an earthquake, some members may undergo stresses of plastic range. These plastic stresses may cause low cycle fatigue (LCF) damage during the earthquake while subjecting to HCF in service conditions. This combined damage of HCF and LCF may be a reason for much reduced life than that predicted by HCF alone (Kondo and Okuya, 2007). Therefore, it is important to study life estimation methods based on combined damage of HCF and LCF to prevent unexpected failures of such bridges in the future.

Most of available literature on fatigue life estimation of steel bridges is focused on HCF caused by usual traffic loading (Mori et al., 2007; Righiniotis et al., 2008; Caglayan et al., 2009; Pipinato et al., 2009). To the knowledge of authors, there exists a considerable lack of information regarding the combined damage of HCF and LCF of bridges. However, in fields such as aircraft and

mechanical engineering, combined damage of HCF and LCF has considerably been studied (Oakley and Nowell, 2007; Hou et al., 2009; Colin and Fatami, 2010). There, Coffin-Manson strain-life curve (total strain-amplitude versus number of reversals to failure) is generally used with Miner's rule (Miner, 1945) as the method to estimate the life for combined damage of HCF and LCF (Suresh, 1998) since it can be used easily to estimate life of components. This method gives better predictions in situations where HCF damage is lower than LCF damage. Recently, a more accurate method (Kim et al., 2009) has been proposed to estimate combined damage of HCF and LCF where HCF damage is higher than LCF damage. This approach is based on a modified Coffin-Manson curve and the Miner's rule.

The modification of Coffin-Manson curve is made by changing the slope of the original curve in the HCF regime to take account of damage interaction effect and damage below the fatigue limit. The factors which are used to modify the slope of the curve depend on the particular materials and these are not readily available for majority of materials. Therefore, obtaining the modified Coffin-Manson curve is difficult for majority of materials.

Miner's rule is the simplest and most widely used fatigue life prediction technique. One of its interesting features is that life calculation is simple and reliable when the detailed loading history is unknown. However under much variable amplitude loading conditions, Miner's rule based on life predictions have been found to be unreliable since it cannot capture loading sequence effect

---

\*Corresponding author. E-mail: [kamal@cee.ehime-u.ac.jp](mailto:kamal@cee.ehime-u.ac.jp). Tel: 81 90 3169 9064. Fax: 81 90 3169 9064.

(Mesmacque et al., 2005; Siriwardane et al., 2007, 2008).

Since bridges are subjected to variable amplitude loading, the use of Miner's rule may give inaccurate life predictions. Therefore, these reasons restrict the application of this method (Kim et al., 2009) to life estimation for combined damage of HCF and LCF in bridges which are generally subjected to variable amplitude loading and higher HCF damage.

The studies (Mesmacque et al., 2005; Siriwardane et al., 2007, 2008) were conducted with a new damage indicator that can capture loading sequence effect in HCF regime. Especially, the studies of (Siriwardane et al., 2007, 2008) explain the results of an existing bridge in HCF regime. However, its direct application for combined damage is inaccurate since combined damage is more complex and different from the situation of only HCF presence (Lanning et al., 2001).

Therefore, it is necessary to have a different model, which is based on commonly available material properties, to estimate more accurately the life for combined damage of HCF and LCF due to variable amplitude loadings.

The objective of this paper is to propose a new model to estimate the fatigue life for combined damage of HCF and LCF due to variable amplitude loading conditions. The model consists of a new damage indicator and strain-life curve and these are original points of this paper. The new damage indicator can accurately capture the loading sequence effect. The strain-life curve caters with new damage indicator for better estimation of combined damage of HCF and LCF. The model can be applied to a wide range of materials since it depends on commonly available material parameters.

First, the paper proposes the new fatigue model. Verification of the model is then performed by comparing it with experimental fatigue lives and theoretical predictions. Finally, the model is applied to estimate the fatigue life of a bridge member for combined damage of HCF and LCF caused by usual traffic and earthquake loadings.

## PROPOSED FATIGUE MODEL

This section proposes the new fatigue model to estimate life of steel structures for combined damage of HCF and LCF due to variable amplitude loading. Total strain is considered as the damage variable in the proposed model. Initially, the details relevant to proposed strain-life fatigue curve are discussed. Then, the section clearly describes the proposed damage indicator.

### Strain-life fatigue curve

Summation of independent damages of HCF and LCF does not directly represent real damage behaviour for combined damage of HCF and LCF (Constantinescu et al., 2003). To take into account the damage dependent effect in combined HCF and LCF, it is necessary to modify the strain-life fatigue curve in HCF regime. This, together with the requirement of hypothetical ultimate strain in HCF regime for the proposed damage indicator (damage indicator) leads to construct of a full range of different strain-life curve for HCF

regime in addition to the strain-life curve used in LCF regime. In this paper, the damage transfer technique proposed by Mesmacque et al. (2005) is used for combined damage of HCF and LCF. However, strain is used as the damage variable for both HCF and LCF regimes.

The proposed curve consists of two parts as shown in Figure 1. The first part of the curve describes fatigue life of plastic strain cycles ( $\epsilon \geq \epsilon_y$ ) which usually affect LCF and the second part for elastic strain cycles ( $\epsilon < \epsilon_y$ ) which usually affect HCF. To describe the first part, Coffin-Manson strain-life curve is utilized as shown.

$$\epsilon = \frac{\sigma_f'}{E} (2N)^b + \epsilon_f' (2N)^c \quad (1)$$

Where  $\epsilon$  is the applied strain amplitude,  $N$  is the number of cycles to failure,  $\sigma_f'$  is the fatigue strength coefficient,  $b$  is the fatigue strength exponent,  $\epsilon_f'$  is the fatigue ductility coefficient,  $c$  is the fatigue ductility exponent and  $E$  is the elastic modulus of the material.

The ultimate strain of low cycle fatigue ( $\epsilon$ )<sub>ULCF</sub> which is the total strain amplitude corresponding to failure in half reversal (a quarter of a cycle) is obtained from equation (1) as,

$$(\epsilon)_{ULCF} = \epsilon_f' \quad (2)$$

These parameters are generally known for most materials and can be found in the literature. Therefore, the first part of the curve can be obtained for most materials easily without conducting additional material test.

The second part of the curve, as mentioned earlier, describes the fatigue life of elastic strain cycles ( $\epsilon < \epsilon_y$ ) which usually affects HCF. This part of the curve represents hypothetical fully known curve. The shape of the curve is obtained by directly transforming the previous fully known stress-life curve (Siriwardane et al., 2007, 2008) to elastic strain-life curve as shown below.

$$\epsilon = \epsilon_e \left( \frac{N + N_u}{N + N_e} \right)^{b'} \quad (3)$$

Where  $\epsilon_e$  is the strain amplitude of the fatigue limit,  $N_e$  is the number of cycles to failure at strains of  $\epsilon_e$ . The  $\epsilon_y$  and  $N_y$  are the yield strain and the corresponding number of cycles to failure. The  $b'$  is the slope of the finite life region of the curve and it can be determined from the coordinates of points;  $(\epsilon_y, N_y)$  and  $(\epsilon_e, N_e)$ .

The ( $\epsilon$ )<sub>UHCF</sub> is the ultimate strain of high cycle fatigue which is the elastic strain amplitude corresponding to half reversal (a quarter of a cycle) is expressed as,

$$(\epsilon)_{UHCF} = \left( \frac{\sigma_u}{E} \right) \quad (4)$$

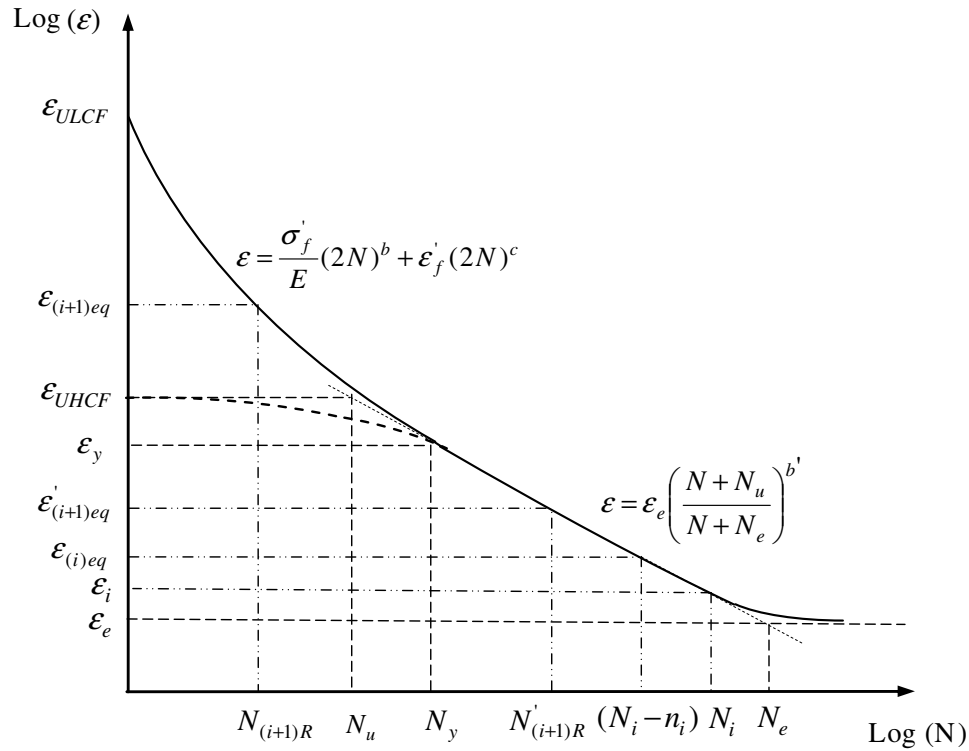


Figure 1. Schematic representation of the proposed strain-life fatigue curve.

where  $\sigma_u$  is the ultimate tensile strength of material. The  $N_u$  is the number cycles corresponding to the intersection of the tangent line of the finite life region and the horizontal asymptote of the ultimate elastic strain amplitude  $(\epsilon)_{UHCF}$  as shown in Figure 1.

Like the first part of the curve, the second part of the curve can be obtained using commonly available parameters without conducting additional material test. Therefore, the proposed strain-life curve can be obtained using commonly available parameters of materials.

### Damage indicator

The proposed damage indicator considers combined damage of HCF and LCF due to variable amplitude loading. The hypothesis behind this fatigue law is that if the physical state of damage is the same, then fatigue life depends only on the loading condition. Suppose a component is subjected to a strain history; a strain amplitude  $(\epsilon)_i$  of  $n_i$  number of cycles at load level  $i$  and a strain amplitude  $(\epsilon)_i$  of  $n_i$  number of cycles at load level  $i$ ,  $N_i$  is the fatigue life (number of cycles to failure) corresponding to  $(\epsilon)_{(i)eq}$  (Figure 1). Therefore, the reduced life at the load level  $i$  is obtained as  $(N_i - n_i)$ . The equivalent strain  $(\epsilon)_{(i)eq}$  (Figure 1), which corresponds to the failure life  $(N_i - n_i)$  is defined as  $i$ th level damage equivalent strain. Hence, the new damage indicator,  $D_i$  is stated as,

$$D_i = \frac{(\epsilon)_{(i)eq} - (\epsilon)_i}{(\epsilon)_u - (\epsilon)_i} \tag{5}$$

where the  $(\epsilon)_u$  is

$$(\epsilon)_u = \begin{cases} \epsilon_{ULCF} & (\epsilon)_i \geq \epsilon_y \\ \epsilon_{UHCF} & (\epsilon)_i < \epsilon_y \end{cases}$$

As shown in Equation (6), the appropriate value for  $(\epsilon)_u$  is selected based on the fatigue regime (HCF or LCF) in which strain amplitude  $(\epsilon)_i$  lies.

This damage  $D_i$  has to be transformed to the next loading level  $i+1$ . It is assumed that at the end of  $i$ th loading level, damage  $D_i$  has been accumulated (occurred) due to the effect of  $(\epsilon)_{i+1}$  loading cycles as follows;

$$D_i = \frac{(\epsilon)_{(i+1)eq} - (\epsilon)_{i+1}}{(\epsilon)_u - (\epsilon)_{i+1}} \tag{7}$$

and  $(\epsilon)_u$  is expressed as

$$(\mathcal{E})_u = \begin{cases} \mathcal{E}_{ULCF} & (\mathcal{E})_{i+1} \geq \mathcal{E}_y \\ \mathcal{E}_{UHCF} & (\mathcal{E})_{i+1} < \mathcal{E}_y \end{cases} \quad (8)$$

Then,  $(\mathcal{E})'_{(i+1)eq}$  is the damage equivalent strain at loading level  $i+1$  and it is calculated as,

$$(\mathcal{E})'_{(i+1)eq} = D_i [(\mathcal{E})_u - (\mathcal{E})_{i+1}] + (\mathcal{E})_{i+1} \quad (9)$$

Thus the corresponding equivalent number of cycles to failure  $N'_{(i+1)R}$  is obtained from the strain-life curve as shown in Figure 1. The  $(\mathcal{E})_{i+1}$  is the strain at the level  $i+1$  and supposing that it is subjected to  $n_{(i+1)}$  number of cycles, then the corresponding residual life at load level  $i+1$ ,  $N_{(i+1)R}$  is calculated as,

$$N_{(i+1)R} = N'_{(i+1)R} - n_{(i+1)} \quad (10)$$

Therefore, strain  $(\mathcal{E})_{(i+1)eq}$ , which corresponds to  $(\mathcal{E})_{(i+1)eq}$  at load level  $i+1$ , is obtained from the strain-life curve as shown in Figure 1. Then the cumulative damage at the end of load level  $i+1$  is defined as,

$$D_{(i+1)} = \frac{(\mathcal{E})_{(i+1)eq} - (\mathcal{E})_{i+1}}{(\mathcal{E})_u - (\mathcal{E})_{i+1}} \quad (11)$$

where  $(\mathcal{E})_u$  is expressed as

$$(\mathcal{E})_u = \begin{cases} \mathcal{E}_{ULCF} & (\mathcal{E})_{i+1} \geq \mathcal{E}_y \\ \mathcal{E}_{UHCF} & (\mathcal{E})_{i+1} < \mathcal{E}_y \end{cases} \quad (12)$$

Similarly, the damage indicator,  $D_i$ , can be calculated for any given strain history. At the first cycle the equivalent strain  $(\mathcal{E})_{(i)eq}$  is equal to  $(\mathcal{E})_i$  and the corresponding damage indicator becomes  $D_i=0$ . Similarly at the last cycle, the damage indicator becomes  $D_i=1$  when  $(\mathcal{E})_{(i)eq}$  is equal to  $(\mathcal{E})_u$ .

Therefore, the damage indicator is normalized to one ( $D_i=1$ ) at the fatigue failure of the material. Hence, the above procedure is followed until  $D_i=1$ . The proposed damage indicator-based algorithm is more clearly summarized in the flow chart shown in Figure 2. Here, the defined fatigue failure is the time taken for initiation of crack at the location of maximum stress of the structural component.

## VERIFICATIONS OF PROPOSED FATIGUE MODEL

In this section, predicted fatigue lives of the proposed model are compared with combined HCF and LCF test

results of two materials and predicted fatigue lives of a precise LCF model. The following subsections describe these comparisons in detail.

### Comparison with experimental lives of combined HCF and LCF tests

The fatigue test results of two materials are compared with the predicted fatigue lives of the proposed model. Two materials are P355NL1 steel (Pereira et al., 2008) and Inconel 718 nickel base super alloy (Cook, 1982). The first material is a low carbon steel which is recommended for manufacturing of pressure equipments. The second material is used in manufacturing of turbines. The tests were performed both in the HCF and LCF regimes under different kinds of variable amplitude loading nature such as increasing or decreasing step loadings, variable amplitude repeating block loadings.

Six fatigue tests of P355NL1 steel were carried out with two steps of strain ranges with values of 1 and 0.5% (Pereira et al., 2008). The specimens were tested under two loading sequences which are increasing (Pattern A) and decreasing (Pattern B) as shown in Figure 3. Three similar types of specimens were tested under each loading sequence. The tests were carried out in such a way that first block is applied for a specified number of cycles, not causing material failure. Then, the second block of loading is applied until the failure is observed. Further, all tests were strain controlled and conducted in null strain ratio. A detailed summary of the tests is given in Table 1.

Failure number of cycles of these tests was predicted by the proposed model. In addition, Miner's rule employed previous model was used to predict the number of cycles to failure. The obtained results are given in Table 1 and plotted in Figure 4. Both models give a close relation of fatigue life for increasing loadings (Pattern A). But predicted lives by previous model differ significantly from experimental lives for decreasing loading (Pattern B). Correlation coefficients of the proposed model predictions and previous model predictions with experimental test results were estimated as 0.97 and 0.64, respectively. The illustrations of Figure 4 and the difference in correlation coefficients convinced us that the proposed method has better correlation with experimental results than Miner's rule employed previous model.

Six fatigue tests (Cook, 1982) of Inconel 718 nickel base super alloy were carried out both under increasing type step loading (Pattern A) and variable amplitude repeating block loading (Pattern B) as shown in Figure 5. The four specimens were tested under increasing type loading with different number steps of strain ranges and two specimens were tested under variable amplitude repeating block loadings (Cook, 1982). A detailed summary of the tests is given in Tables 2 and 3 for increasing type step loading and variable amplitude repeating

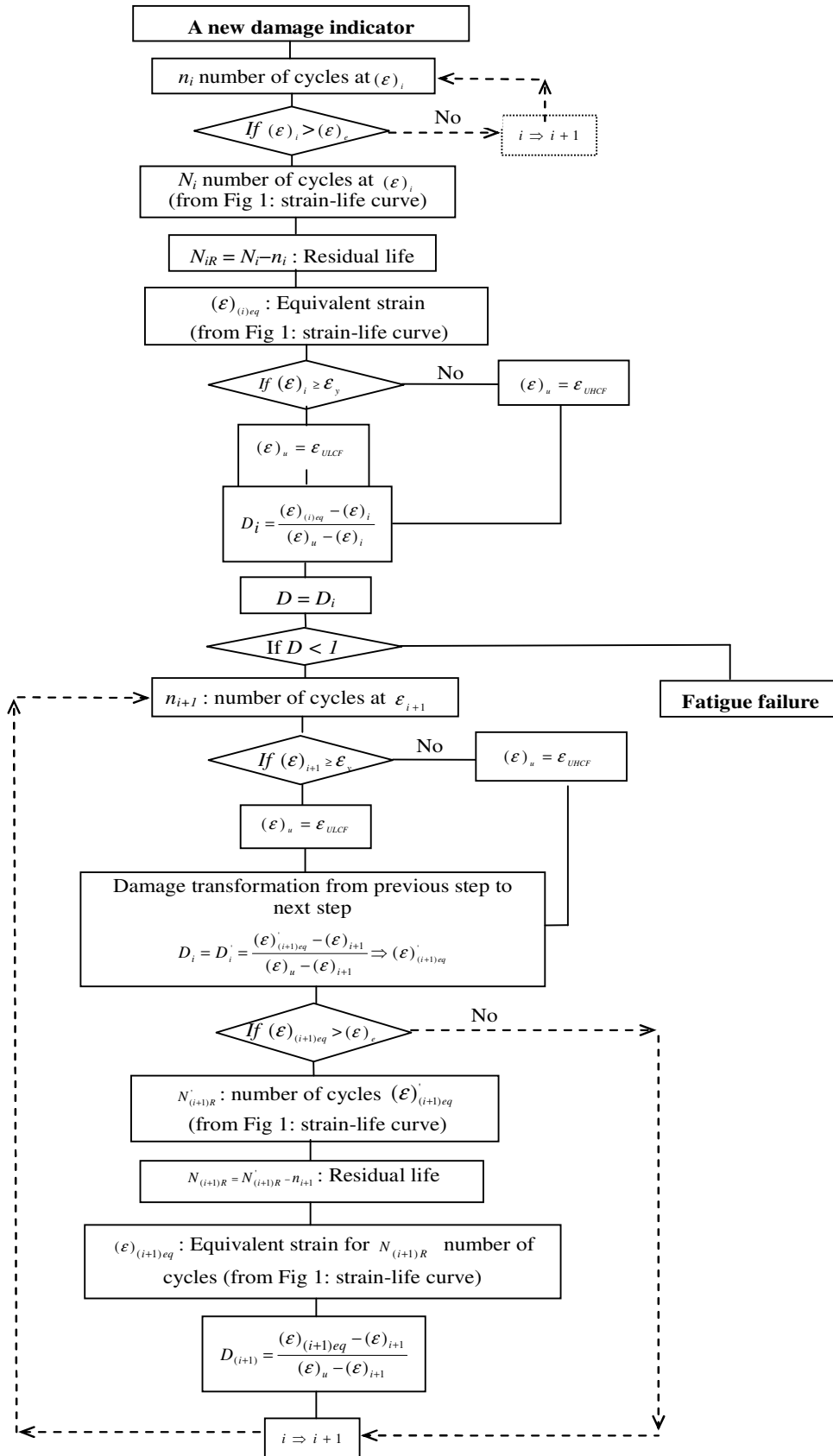
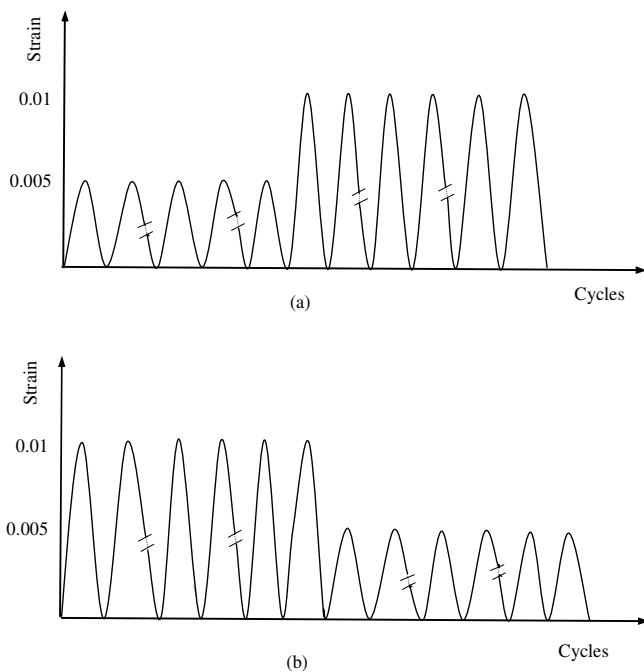


Figure 2. Flow chart of the proposed damage indicator.

**Table 1.** Comparison of predicted lives with experimental lives for P355NL1 steel.

Specimen	First strain step		Second strain step		Experimental fatigue life (cycles)		Predicted fatigue life (cycles)	
	Strain range (%)	Number of cycles ( $n_1$ )	Strain range (%)	Number of cycles ( $n_2$ )	Test result ( $n_1+n_2$ )	Average life	Previous model*	Proposed model
D201	1.0	337	0.5	2525	2862			
D202	1.0	337	0.5	3600	3937	3399	9024	4577
D203	1.0	673	0.5	977	1650			
D204	1.0	673	0.5	2727	3400	2525	5837	2007
D205	1.0	1010	0.5	1790	2800			
D206	1.0	1010	0.5	1404	2414	2607	2641	1805
D301	0.5	3620	1.0	922	4542			
D302	0.5	3620	1.0	1092	4712	4627	4440	4607
D303	0.5	7240	1.0	1507	8747			
D304	0.5	7240	1.0	1044	8284	8515	7715	7972
D305	0.5	9377	1.0	1528	10905			
D306	0.5	9377	1.0	1693	11070	10987	9648	9832

\*: Coffin-Manson curve with Miner's rule.



**Figure 3.** Loading patterns used for P355NL1 steel: (a) Pattern A (increasing loading) (b) Pattern B (decreasing loading).

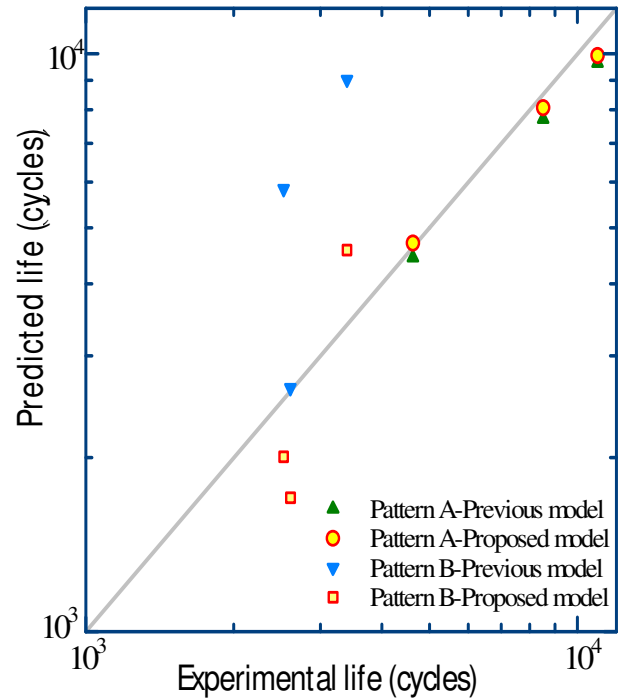


**Figure 4.** Comparison of predicted lives versus experimental lives for P355NL1 steel.

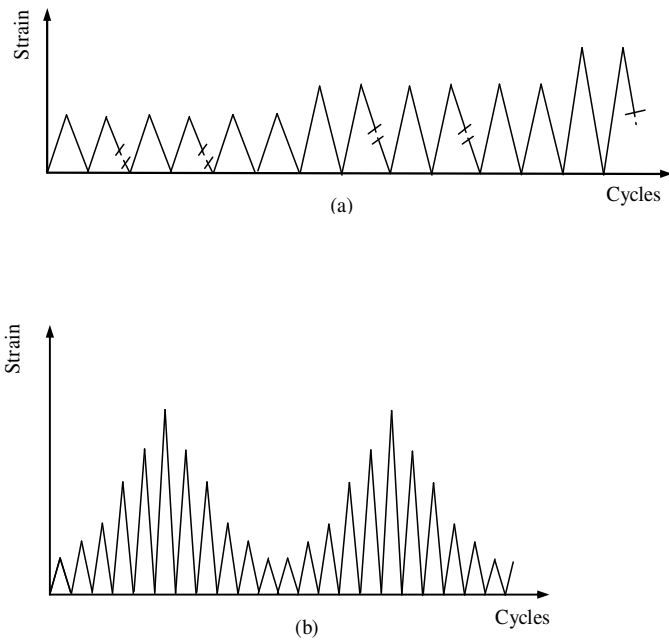


**Figure 5.** Loading patterns used for Inconel 718: (a) Pattern A (increasing type step loading) (b) Pattern B (variable amplitude repeating block loading).

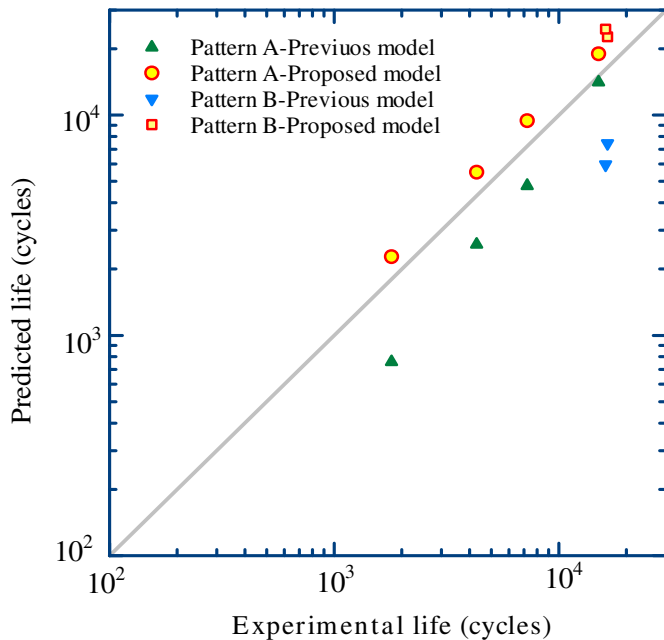


**Figure 6.** Comparison of predicted lives versus experimental lives for Inconel 718.

repeating block loading, respectively. The maximum strain amplitude of each block was subjected to increase in four stages during the strain history.

Failure number of cycles of these tests was predicted by the proposed model. In addition, Miner’s rule employed previous model was used to predict the number of cycles to failure. The obtained results are given in Tables 2 and 3, and plotted in Figure 6. Correlation coefficients of the proposed model predictions and previous model predictions with experimental test results were estimated as 0.99 and 0.76, respectively.

The illustrations of Figure 6 and the difference in correlation coefficients convinced us that the proposed method has better correlation with experimental results than Miner’s rule employed previous model.

**Comparison with predicted lives of a precise LCF model**

Liu et al. (2005) have recently proposed and verified an LCF model for accurate life prediction of A36 steel under variable amplitude loading. The model consists of a new damage indicator which was obtained by modifying the Miner’s rule and considering three multiplication factors such as amplitude change factor, power coefficient for relative strain and partial cycle factor. Further this model describes a new cycle counting method. However, application of this model to other materials was found to be less since model parameter determination procedures are lengthy and difficult. On the other hand, corresponding cycle counting technique for random loading is totally different from well known cycle counting technique such as rain flow or reservoir counting, etc. In this section, this model (Liu et al., 2005) was used to compare with the proposed model prediction in LCF regime. The considered material is A36 steel and four repeating block loading patterns were considered as shown in Figure 7. For each pattern, six different strain history blocks were obtained by varying the amplitude of strain (that is, changing the value “a” of Figure 7 as shown in Table 4). For each history, failure number of cycles was predicted using the proposed model, Liu et al. (2005) model, as well as Miner’s rule employed previous model. The comparisons are given in Table 4 and Figure 8. These comparisons indicate that the proposed model has better correlation with Liu et al. (2005) model for LCF regime than previous model predictions.

**CASE STUDY: FATIGUE LIFE ESTIMATION OF A BRIDGE MEMBER**

Fatigue life estimation of a bridge member is discussed in this section. The purpose of the case study is only to explain the application of the proposed model to an existing bridge member. The evaluations are especially based on secondary stresses and strains, which are generated around the riveted connection of the member due to stress concentration effect of primary stresses caused by usual traffic and earthquake loadings.

**Table 2.** Comparison of predicted lives with experimental lives of Inconel 718 for increasing type step loading.

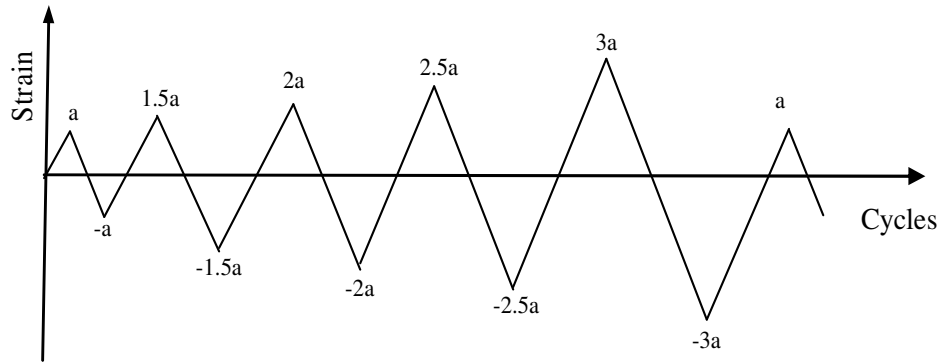
Specimen	Stress range (GPa)	Strain range (%)	$N_i$ (cycles)	Experimental fatigue life (cycles)	Predicted fatigue life (cycles)	
					Previous model*	Proposed model
N-7	1.02	0.5	7600	15040	14102	18959
	1.22	0.6	3400			
	1.44	0.7	1680			
	1.63	0.8	1000			
	1.78	0.9	640			
	1.89	1.0	460			
	1.94	1.1	260			
L-6	1.91	1.1	510	1800	759	2276
	1.94	1.2	360			
	1.97	1.3	290			
	1.98	1.4	220			
	2.00	1.5	170			
	2.03	1.6	140			
	2.02	1.7	110			
N-8	1.63	0.8	2360	4310	2588	5501
	1.86	1.0	1065			
	1.95	1.2	560			
	1.98	1.4	325			
T-7	1.41	0.7	4000	7230	4779	9443
	1.71	0.9	1830			
	1.84	1.1	800			
	1.85	1.2	600			

\*: Coffin-Manson curve with Miner's rule.

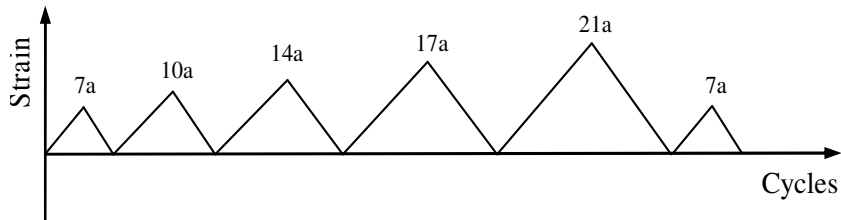
**Table 3.** Comparison of predicted lives with experimental lives of Inconel 718 for variable amplitude repeating block loading.

Specimen	Stress range (GPa)	Strain range	$N$ blocks	Experimental fatigue life (cycles)	Predicted fatigue life (cycles)	
					Previous model*	Proposed model
M-6	1.70	0.9	217	16473	7441	22639
	1.88	1.0	150			
	1.98	1.2	100			
	1.97	1.4	400			
X-7	1.62	0.8	150	16150	5956	24559
	1.93	1.1	150			
	1.89	1.2	150			
	1.89	1.3	400			

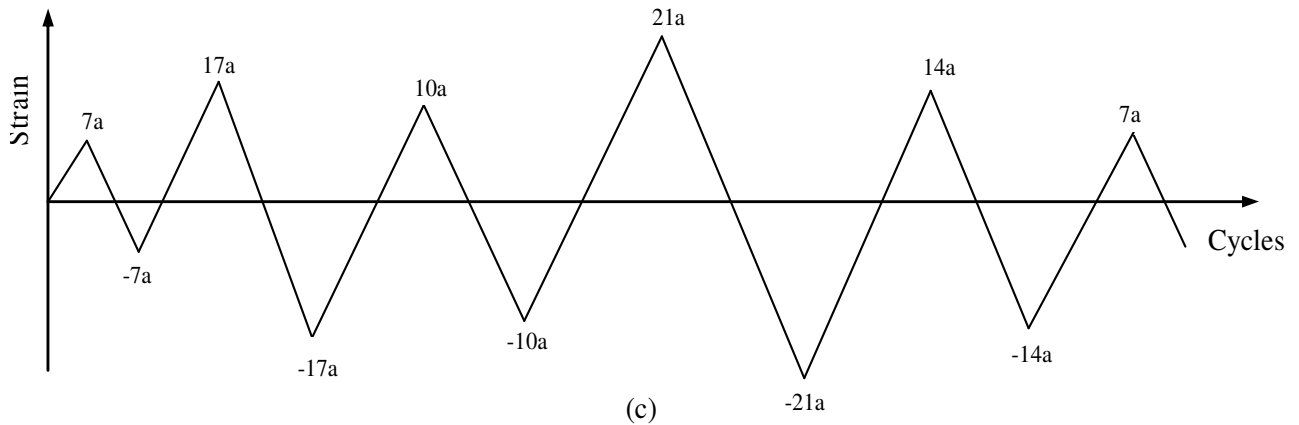
\*: Coffin-Manson curve with Miner's rule



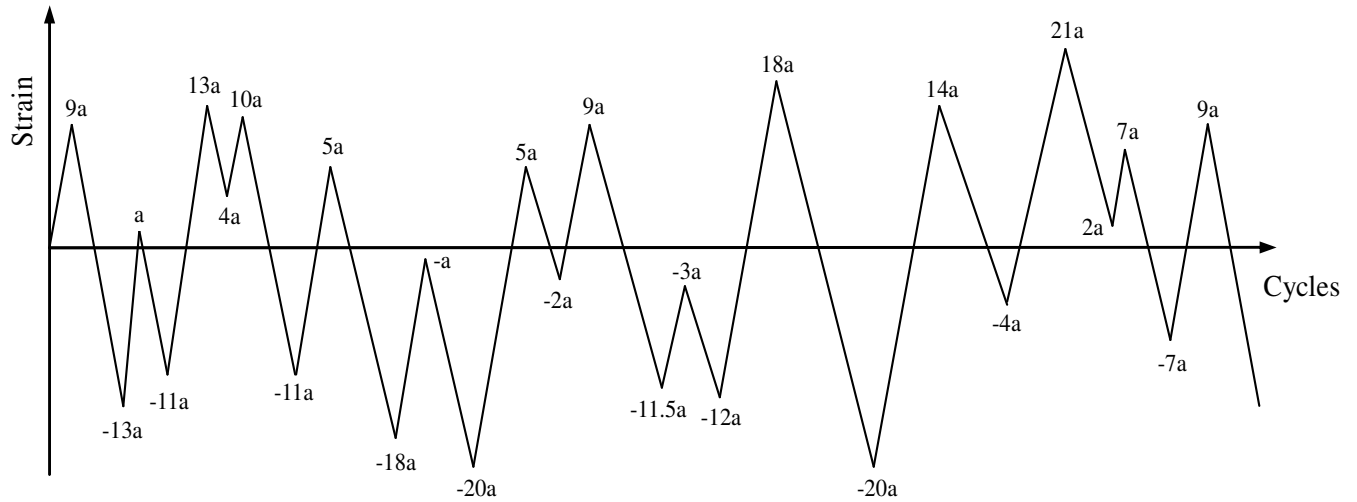
(a)



(b)



(c)



(d)

Figure 7. Loading patterns for A36 steel: (a) Pattern I (b) Pattern II (c) Pattern III (d) Pattern IV.

**Table 4.** Comparison of predicted lives by previous and proposed models with Liu’s life (Liu et al., 2005) for A36 steel.

Pattern	Amplitude magnification factor	Predicted fatigue life (cycles)		
		Liu et al. model	Previous model*	Proposed model
I	0.03	40.5	49	44
	0.0275	54.5	64	58
	0.025	75.5	84	79
	0.0225	108.0	119	111
	0.02	159.0	173	162
	0.015	399.0	427	403
II	0.0045	33.0	43	38
	0.004	49.5	61	56
	0.0035	80.0	93	86
	0.003	136.5	153	142
	0.0025	251.0	271	254
	0.002	523.0	548	517
III	0.0055	31.5	51	43
	0.005	43.0	74	59
	0.0045	63.0	101	82
	0.004	92.5	140	119
	0.0035	141.5	209	182
	0.003	232.5	342	298
IV	0.0025	414.5	608	532
	0.0055	35.5	70	58
	0.005	52.5	89	76
	0.004	113.0	178	154
	0.0035	179.0	268	236
	0.003	299.5	434	384
	0.0025	542.5	764	684

\*: Coffin-Manson curve with Miner’s rule.

The considered bridge is one of the longest and busiest railway bridges in Sri Lanka situated near Colombo and carries the main railway line of the country. It was constructed in 1885 and since then it has been in operation without any major structural alterations except some strengthening conducted in 1939. A view of the bridge is shown in Figure 9a.

The bridge is semi-through having 6 double-system Warren girders supported on cylindrical piers. Its length, height and width are 154.8, 13.5 and 8.85 m, respectively and consisting of 6 spans. The super structure is made of wrought iron and the substructure is cast iron casings within filled concrete. The present service load varies from 28.86 to 112.8 tons.

**Considered member**

A structural appraisal was carried recently by University of Peradeniya (Ranaweera et al., 2002) in response to the request made by Sri Lankan Railway to find out current serviceable condition of the bridge. The visual,

experimental and analytical investigation of the study led us to perceive the present condition of the bridge and identify critical members of the bridge. It was understood that a particular bracing member is highly subjective for fatigue failure. In history, it has been noticed that some of these types of members have failed but the reason is not yet known. Further, previous time-history analysis of the global structure of the bridge revealed that this member is also the one of highly stressed members for earthquake loadings. Therefore, that member was selected for fatigue life estimation to explain the application of the proposed model. A view of the selected member is shown in Figure 9b.

**Stress-strain analysis**

The combined damage of HCF and LCF is evaluated based on the state of strain due to release of contact (tightness) of rivets while all the riveted locations have no clamping force. The clamping force is generally defined as the compressive force in the plates which is induced

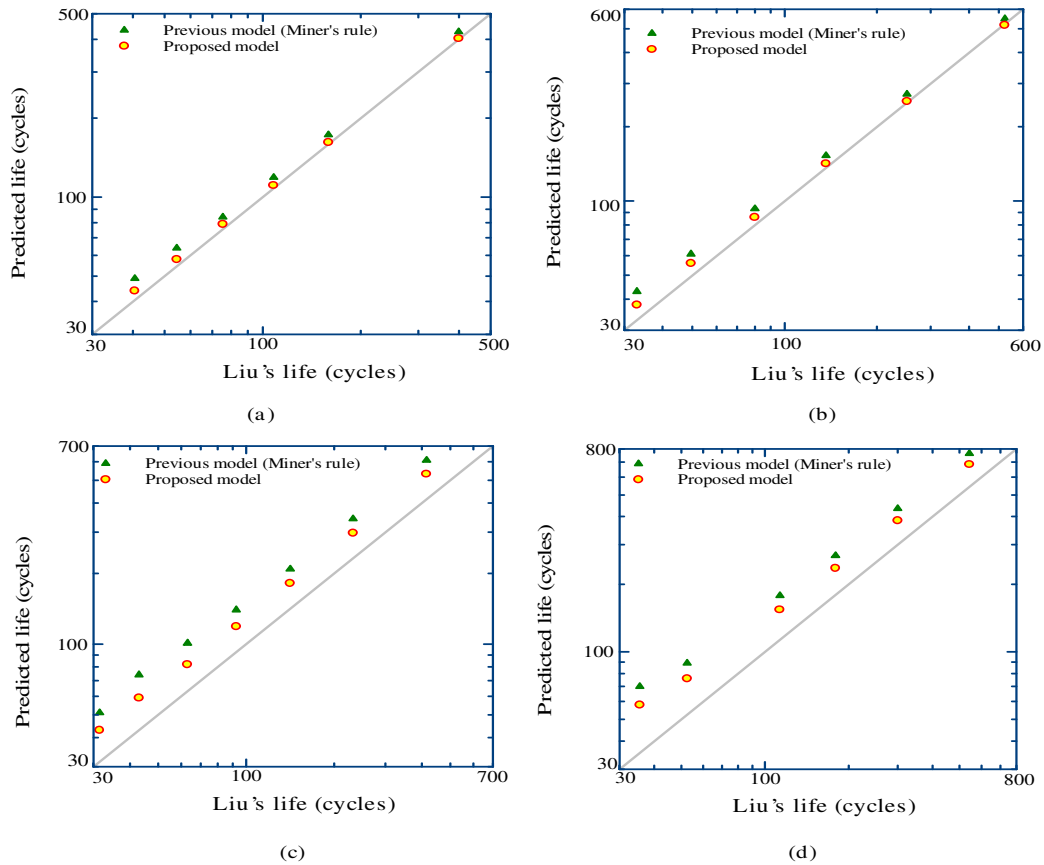


**Figure 8.** Comparison of predicted lives versus Liu's lives (Liu et al. 2005) for: (a) Loading pattern I (b) Loading pattern II (c) Loading pattern III (d) Loading pattern IV.

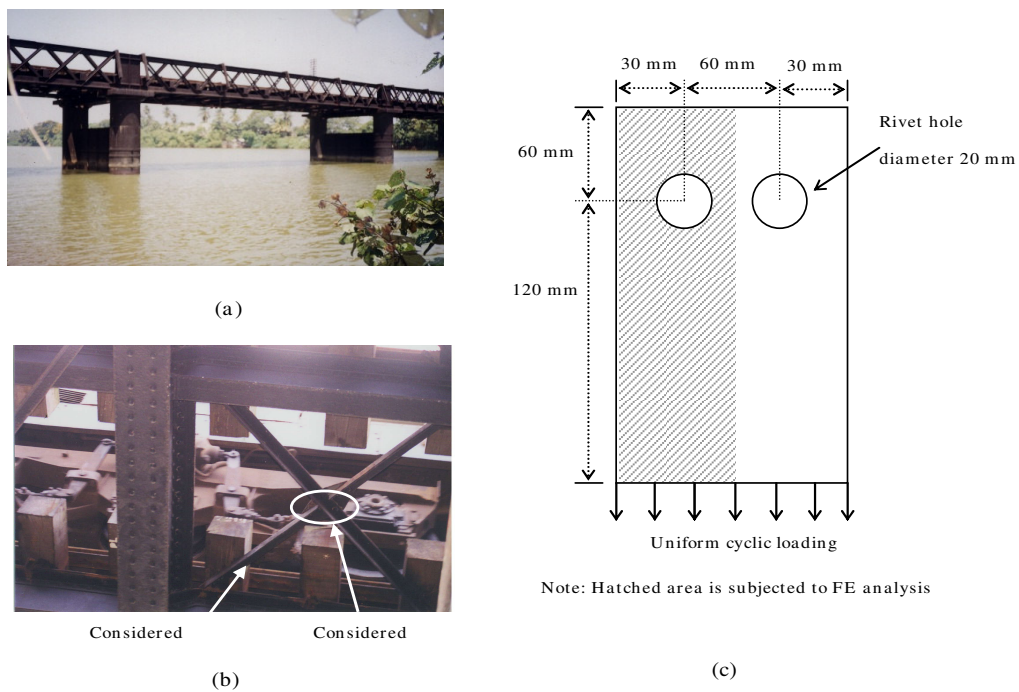


**Figure 9.** Considered member: (a) General view of the bridge, (b) Close view of considered connection and member, (c) Geometric details of connection.

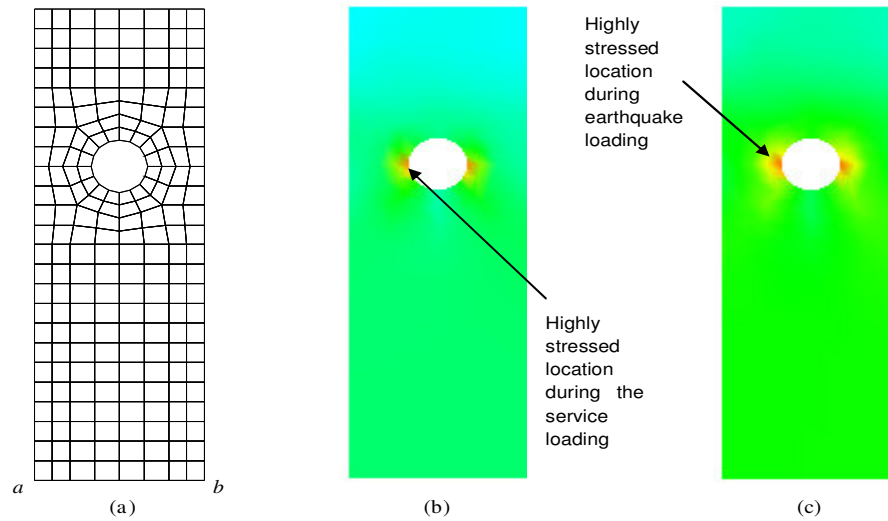


**Figure 10.** Stress analysis: (a) FEM mesh (b) Maximum von Mises stress distribution during service loading (c) Maximum von Mises stress distribution during earthquake loading.

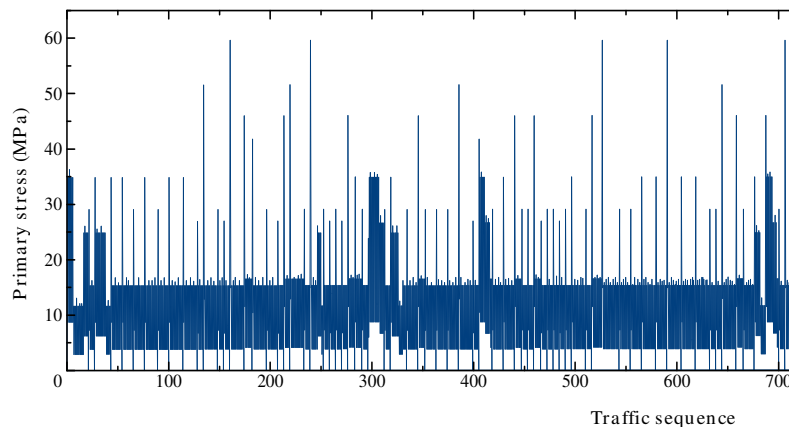


**Figure 11.** Primary stress variation of the member with traffic sequence per single day.

by the residual tensile force in the rivet. The residual force in the rivets occurs when the rivet get shortened in length due to cooling after a hot rivet is inserted into the hole of plates in order to connect them, and a second head is formed from the protruding shank. Finally clamping force generates a triaxial state of stress in the connected plate (Siriwardane et al., 2007; 2008). Since this study assumes that the riveted locations have no clamping force (value of clamping force is zero), the connected members are considered to subject to the biaxial stress state. Therefore, a critical member without rivets can be considered to analyze the biaxial state of stress. Considering symmetry, one half (hatched area) of the member was considered for FE analysis shown in Figure 9c. A FEM program with a FORTRAN source code which

was developed in Ehime University was used in FE analysis. It can accurately model elastic and elasto-plastic behavior of materials. The nine node isoperimetric shell elements were used for the finite element analysis as shown in Figure 10a. The actual air gap restraint conditions were considered in the model to represent unilateral contact between the rivet and the plate. To make the continuity of the stress field between the global structure and the sub structure, it is required to use any interface between the two structures at every iterative step. Therefore, in this model, primary tensile stress history (Figure 11) of the member, which has been obtained from measured strain histories at the mid span of the bridge due to usual traffic loadings (Figure 11), is applied to the bottom face as uniform pressure. The position of

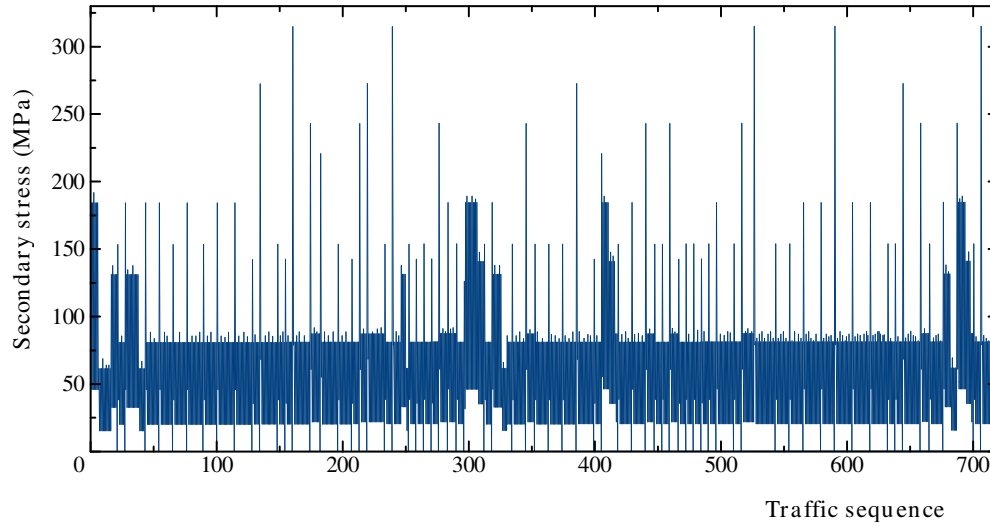


**Figure 12.** Secondary stress variation of the critical location with traffic sequence per single day.

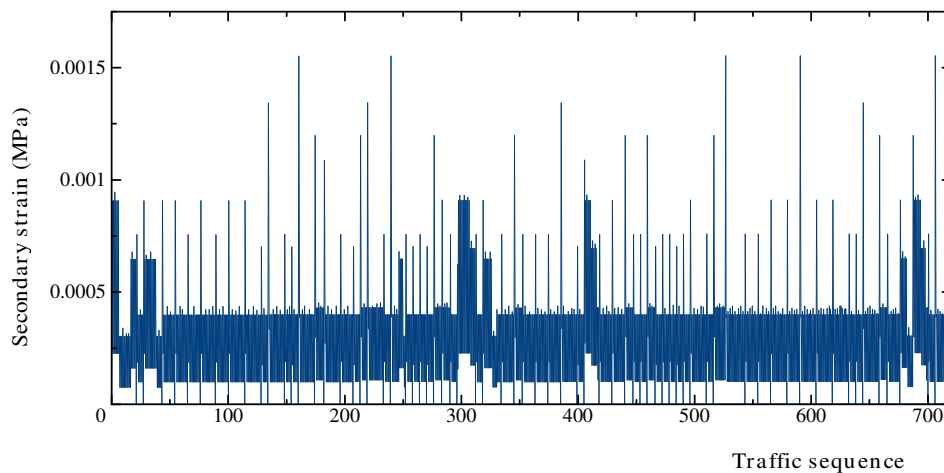


**Figure 13.** Secondary strain variation of the critical location with traffic sequence per single day.

position of the ab boundary of the sub model was determined considering the distribution of the far field primary stress of the member. The obtained maximum stress contours are shown in Figure 10b. This shows that stresses are operating well below the yield limit of the material (therefore HCF regime) and the highly stressed locations are subjected to uniaxial stress state. Assuming that a single day traffic sequence is repeating every day, one day time history is considered as the loading block in this study. The obtained secondary stress and strain histories for normal traffic loadings are shown in Figures 12 and 13 respectively.

In this case study, fatigue life was calculated for combined damage of usual traffic and earthquake loadings. Therefore, the same geometry of the member is subjected to further analysis assuming it is subjected to

an earthquake loading. Then the elasto-plastic analysis was conducted by applying the primary stress history (Figure 14) which was obtained by time history analysis of global structure under earthquake loading was applied to the ab interface as same as above. The obtained maximum stress contours are shown in Figure 10c and it was decided that state of stress is uniaxial. The obtained secondary stress and strain histories for earthquake loadings are shown in Figures 15 and 16, respectively.

The obtained secondary strain variations (Figures 13 and 16) are complex and also of irregular shape. These strains should be reduced to a series of equivalent strain cycles at zero mean strain. In order to achieve this objective, initially the famous rainflow cycle counting technique (Dowling and Socie, 1982) is used to identify the strain ranges and sequences of closed strain cycles.

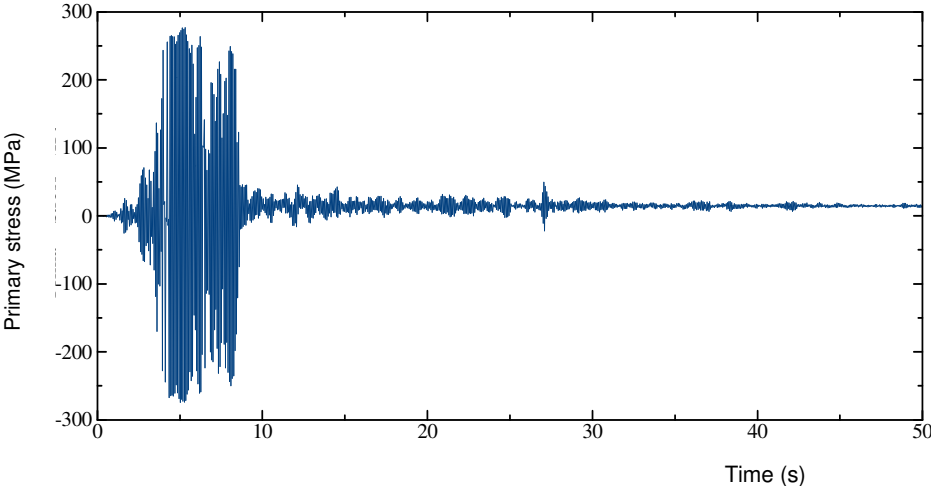


Figure 14. Primary stress history of the member during the earthquake.

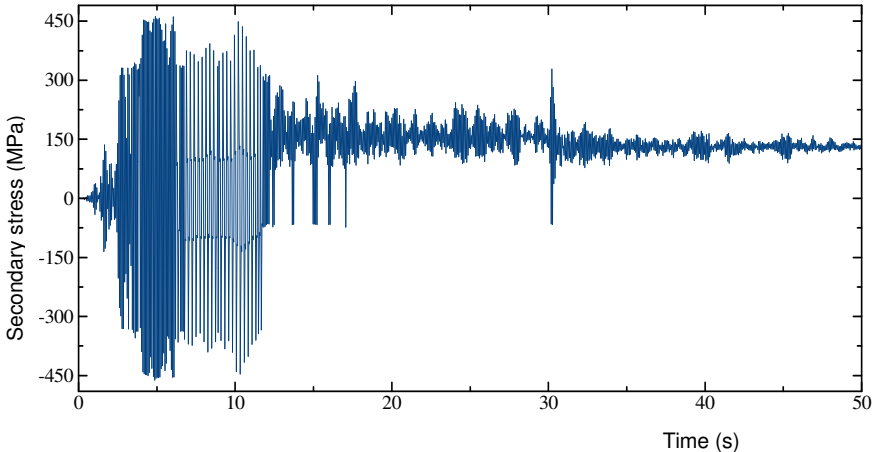


Figure 15. Secondary stress history of the critical location during the earthquake.

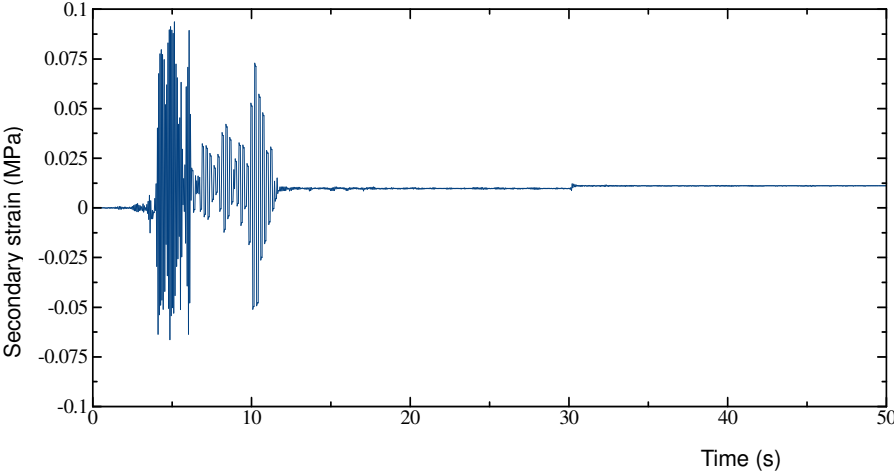
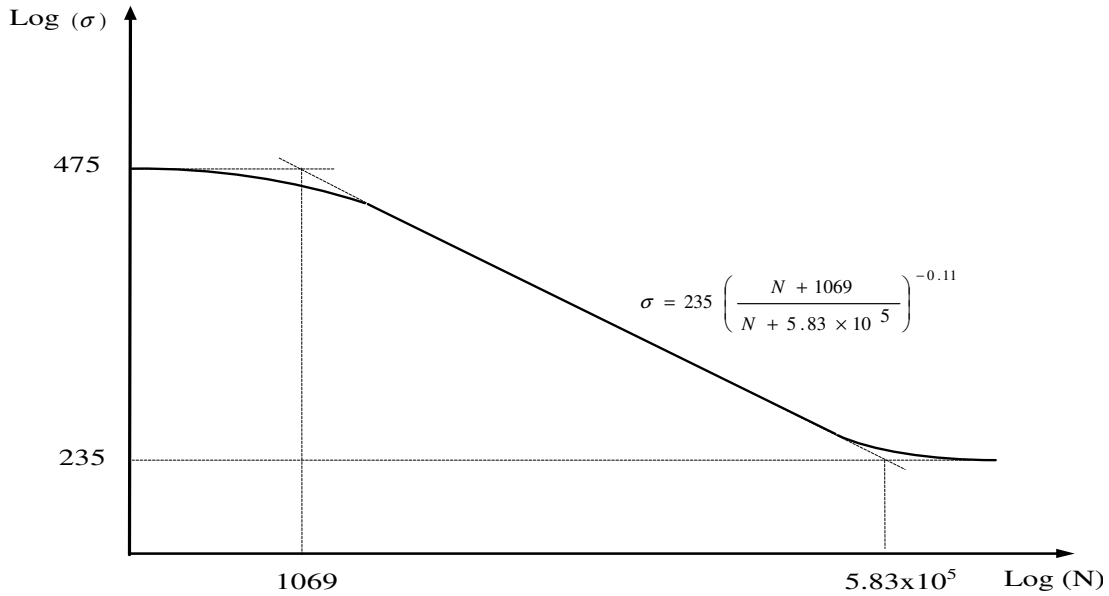
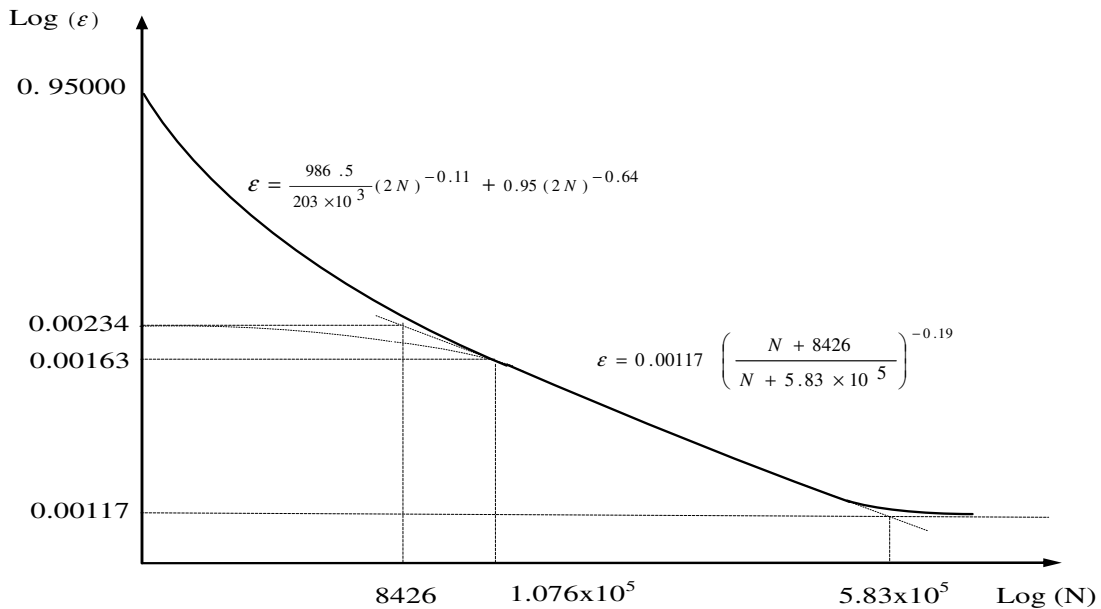


Figure 16. Secondary strain history of the critical location during the earthquake.



(a)



(b)

**Figure 17.** Fatigue curves for considered bridge material for use (a) Before the earthquake (b) During and after the earthquake.

Then modified Goodman relation is used to transfer these counted cycles to mean strain zero stabilized cycles.

**Fatigue curves**

Fatigue properties,  $\sigma_f'$ ,  $b$ ,  $\epsilon_f'$ ,  $c$ ,  $\sigma_y$ ,  $\sigma_u$ ,  $\sigma_e$  and  $E$  of the considered member are 986.5 MPa, -0.11, 0.95, -0.64, 330 MPa, 475 MPa, 235 MPa and 203 GPa, respectively.

From these properties,  $\epsilon_{ULCF}$ ,  $\epsilon_{UHCF}$ ,  $\epsilon_y$ ,  $\epsilon_e$ ,  $N_y$  and  $N_e$  are estimated as 0.95, 0.00234, 0.00163, 0.00117,  $1.076 \times 10^5$  and  $5.83 \times 10^5$  respectively as explained in the strain-life fatigue curve. Then,  $b'$  and  $N_u$  were estimated as -0.19 and 8426, respectively (strain-life fatigue curve). From these parameters, the corresponding stress-life curve for HCF and the strain-life curve for combined HCF and LCF of the considered bridge material are constructed as shown in Figure 17.

**Table 5.** Comparison of calculated fatigue lives of the riveted connection.

Time of earthquake* (years)	Previous model (Miner's rule)		Proposed curve with Miner's rule		Proposed model	
	Fatigue life (years)	Percentage reduction of life (%)	Fatigue life (years)	Percentage reduction of life (%)	Fatigue life (years)	Percentage reduction of life (%)
5	26.5	35.4	34.0	17.0	22.0	63.3
10	26.5	35.4	34.0	17.0	24.0	60.0
20	26.5	35.4	34.0	17.0	29.0	51.7
30	30.0	26.8	34.0	17.0	34.0	43.3
40	40.0	2.4	-	-	41.0	31.7
50	-	-	-	-	50.5	15.8
54	-	-	-	-	54.0	10.0
Without earthquake	41.0	-	41.0	-	60.0	-

\*: After construction.

### Fatigue life estimation

Until the earthquake occurrence, the damage due to usual traffic loads (HCF) was evaluated using a previously proposed HCF model (Siriwardane et al., 2008) with the stress-life curve shown in Figure 17a. During and after the earthquake, fatigue damage was evaluated using the proposed combined HCF and LCF model (Proposed fatigue model). The updated damage (damage accumulation) was calculated by following the flow chart given in Figure 2. The fatigue life was estimated when the damage indicator reaches to the unity.

Earthquake was considered to occur at different times of the bridge life such as 5, 10, 20, 30, 40, 50 and 54 years as shown in Table 5. It is assumed that usual traffic load is followed after the earthquake until the member failure. The fatigue life of the member was estimated using three approaches: (1) proposed model; (2) previous model; (3) The Miner's rule with the proposed strain-life curve. The purpose of using approach (3) was to estimate the effect of the proposed strain-life curve on life estimation instead of Coffin Manson strain relationship.

The obtained results are given in Table 5 for three approaches. The results indicate that LCF damage by earthquake loading causes an appreciable reduction of bridge life. For the proposed model, percentage reduction of life is higher when the earthquake occurs at the beginning of the bridge life compared to those occurring in later times. For example, when the earthquake occurs 5 years after construction, the previous model predicts the fatigue life as 26.5 years causing 35.4% of life reduction. However, the proposed model gives a fatigue life as 22.0 years causing 63% of life reduction. When the earthquake occurs later in the bridge life, percentage reduction of the service life gets lower for the proposed model. However, Miner rule gives a constant percentage reduction of service life since it cannot capture the

loading sequence effect. The amount of fatigue damage predicted by the Miner's rule is constant irrespective of its occurrence time. The results obtained using Miner's rule with the proposed curve (approach 3) lies between the previous and the proposed methods. Therefore, it indicates that the proposed curve more accurately represent the combined damage of HCF and LCF than the Coffin Manson strain relationship. The differences in case study results confirm the importance of accurate combined HCF and LCF model to estimate the fatigue life of existing connections.

### Conclusion

A new model for combined damage of HCF and LCF was proposed to estimate the fatigue life of steel structures such as bridges. A verification of the model was conducted by comparing the predicted lives with experimental lives due to variable amplitude loading for two materials available in the literature. Further, the model was verified with a previously proposed model only in LCF regime. It was shown that the proposed fatigue model gives a realistic fatigue life for the combined damage of HCF and LCF in variable amplitude loading situations where detailed stress histories are known. The proposed fatigue model was used to estimate the fatigue life of a bridge member of an old wrought iron railway bridge. Case study realized the importance of consideration of the earthquake induced LCF damage in addition to HCF damage due to usual traffic loading in steel bridges. The importance of accurate prediction of combined damage of HCF and LCF was also confirmed. Further verifications of proposed model in more complex loading situations are currently under way. Since this model only describes the uniaxial stress state, it is recommended to extend these models for multiaxial stress state in the future.

## ACKNOWLEDGEMENTS

The authors wish to express their sincere gratitude to Professor M.P. Ranaweera and the team of experts who worked in the Sri Lankan Railway Bridge project, for their great advice in carrying out this research. The kind support given by the Sri Lanka Railways (SLR) is also appreciated.

## REFERENCES

- Caglayan BO, Ozakgul K, Tezer O (2009). Fatigue life estimation of a through girder steel railway bridge, *Eng. Failure Anal.*, 16(3): 765-774.
- Chen WF, Lui EM (1987). *Handbook of Structural Engineering*. CRC Press, New York.
- Colin J, Fatami A (2010). Variable amplitude cyclic deformation and fatigue behavior of stainless steel 304L including step, periodic, and random loadings, *Fatigue Fracture Eng. Materials Structures*. 33(4): 205-220.
- Constantinescu A, Van KD, Maitournam MH (2003). A unified approach for high and low cycle fatigue based on shakedown concepts. *Fatigue and Fracture of Eng. Materials Structures*, 26(6): 561-568.
- Cook TS (1982). Stress-strain behavior of Inconel 718 during low cycle fatigue. *J. Eng. Materials Technol.*, 104(3): 186-191.
- Dowling SD, Socie DF (1982). Simple rainflow counting algorithms, *Int. J. Fatigue*, 4(1): 31-40.
- Hou NX, Wen ZX, Yu QM, Yue ZF (2009). Application of a combined high and low cycle fatigue life model on life prediction of SC blades, *Int. J. Fatigue*, 31(4): 616-619.
- Kim YH, Song JH, Park JH (2009). Expert system for fatigue life prediction under variable loading, *Expert Syst. Appl.*, 36(3): 4996-5008.
- Kondo Y, Okuya K (2007). The effect of seismic loading on the fatigue strength of welded joints, *Material Sci. Eng. A.*, 468-470: 223-229.
- Lanning D, Haritos GK, Nicholas T, Maxwell DC (2001). Low cycle fatigue/high cycle fatigue interactions in notched Ti-6Al-4V, *Fatigue Fracture Eng. Materials Structures*, 24(12): 565-577.
- Liu W, Liang Z, Lee G (2005). Low cycle bending fatigue of steel bars under random excitation. Part II: design considerations. *J. Structural Eng.*, 131(6): 919-923.
- Mesmacque G, Garcia S, Amrouche A, Rubio-Gonzalez C (2005). Sequential law in multiaxial fatigue, a new damage indicator, *Int. J. Fatigue*, 27(4): 461-467.
- Miner MA (1945). Cumulative damage in fatigue. *J. Appl. Mechanics*, 12: 159-64.
- Mori T, Lee H, Kyung K (2007). Fatigue life estimation parameter for short and medium span steel highway girder bridges, *Eng. Structures*, 29(10): 2762-2774.
- Oakley SY, Nowell D (2007). Prediction of the combined high- and low cycle fatigue performance of gas turbine blades after foreign object damage, *Int. J. Fatigue*, 29(1): 69-80.
- Pereira HFSG, de Jesus AMP, Fernandes AA, Ribeiro AS (2008). Analysis of fatigue damage under block loading in a low carbon steel, *Strain*, 44(6): 429-439.
- Pipinato A, Pellegrino C, Bursi OS, Modena C (2009). High cycle fatigue behavior of riveted connections for railway metal bridges, *J. Constructional Steel Res.*, 65(12): 2167-2175.
- Ranaweera MP, Aberuwan H, Mauroof ALM, Herath KRB, Dissanayake PBR, Siriwardane, SASC, Adasooriya AMND (2002). Structural appraisal of Railway Bridge at Colombo over Kelani River, Engineering Design Centre, University of Peradeniya.
- Righiniotis TD, Imam BM, Chryssanthopoulos MK (2008). Fatigue analysis of riveted railway bridge connections using theory of critical distances. *Eng. Structures*, 30(10): 2707-2715.
- Siriwardane S, Ohga M, Dissanayake R, Taniwaki K. (2008). Application of new damage indicator-based sequential law for remaining fatigue life estimation of railway bridges, *J. Constructional Steel Res.*, 64(2): 228-237.
- Siriwardane SC, Ohga M, Dissanayake R, Taniwaki K (2007). Different approaches for remaining fatigue life estimation of critical members in railway bridges, *Int. J. Steel Structures*, 7(4): 263-276.
- Suresh S (1998). *Fatigue of materials*. UK: Cambridge University Press, Cambridge.